



# Open Research Online

---

The Open University's repository of research publications and other research outputs

## 2-16 $\mu\text{m}$ spectroscopy of micron-sized enstatite $(\text{Mg,Fe})_2\text{Si}_2\text{O}_6$ silicates from primitive chondritic meteorites

### Journal Item

How to cite:

Bowey, J. E.; Morlok, A.; Kohler, M. and Grady, M. (2007). 2-16  $\mu\text{m}$  spectroscopy of micron-sized enstatite  $(\text{Mg,Fe})_2\text{Si}_2\text{O}_6$  silicates from primitive chondritic meteorites. *Monthly Notices of the Royal Astronomical Society*, 376(3) pp. 1367–1374.

For guidance on citations see [FAQs](#).

© [\[not recorded\]](#)

Version: [\[not recorded\]](#)

Link(s) to article on publisher's website:  
<http://dx.doi.org/doi:10.1111/j.1365-2966.2007.11548.x>

---

Copyright and Moral Rights for the articles on this site are retained by the individual authors and/or other copyright owners. For more information on Open Research Online's data [policy](#) on reuse of materials please consult the policies page.

---

[oro.open.ac.uk](http://oro.open.ac.uk)

## 2–16 $\mu\text{m}$ spectroscopy of micron-sized enstatite $(\text{Mg,Fe})_2\text{Si}_2\text{O}_6$ silicates from primitive chondritic meteorites

J. E. Bowey,<sup>1\*</sup> A. Morlok,<sup>2†</sup> M. Köhler<sup>2,3</sup> and M. Grady<sup>2,4</sup>

<sup>1</sup>*Department of Physics and Astronomy, University College London, Gower Street, London WC1E 6BT*

<sup>2</sup>*Department of Mineralogy, The Natural History Museum, Cromwell Road, London SW7 5BD*

<sup>3</sup>*Institut für Planetologie, Wilhelm-Klemm-Str. 10, 48149 Münster, Germany*

<sup>4</sup>*PSSRI, The Open University, Walton Hall, Milton Keynes MK7 6AA*

Accepted 2007 January 22. Received 2007 January 22; in original form 2006 March 1

### ABSTRACT

We present mid-infrared spectra from individual enstatite silicate grains separated from primitive type 3 chondritic meteorites. The 2–16  $\mu\text{m}$  transmission spectra were taken with microspectroscopic Fourier-transform infrared (FT-IR) techniques as part of a project to produce a data base of infrared spectra from minerals of primitive meteorites for comparison with astronomical spectra. In general, the wavelength of enstatite bands increases with the proportion of Fe. However, the wavelengths of the strong  $\text{En}_{100}$  bands at 10.67 and 11.67  $\mu\text{m}$  decrease with increasing Fe content. The 11.67- $\mu\text{m}$  band exhibits the largest compositional wavelength shift (twice as large as any other). Our fits of the linear dependence of the pyroxene peaks indicate that crystalline silicate peaks in the 10- $\mu\text{m}$  spectra of Herbig AeBe stars, HD 179218 and 104237, are matched by pyroxenes of  $\text{En}_{90-92}$  and  $\text{En}_{78-80}$ , respectively. If these simplistic comparisons with the astronomical grains are correct, then the enstatite pyroxenes seen in these environments are more Fe-rich than are the forsterite ( $\text{Fo}_{100}$ ) grains identified in the far-infrared which are found to be Mg end-member grains. This differs from the general composition of type 3 chondritic meteoritic grains in which the pyroxenes are more Mg-rich than are the olivines from the same meteorite.

**Key words:** circumstellar matter – infrared: stars.

### 1 INTRODUCTION

The ubiquity of dust (interstellar, circumstellar, interplanetary, cometary and asteroidal) is an indication of its importance in a variety of astrophysical environments. The accepted astronomical view is that the majority of this dust is amorphous and relatively homogeneous because mid-IR (10 and 18  $\mu\text{m}$ ) spectroscopy of oxygen-rich dust in a variety of galactic environments reveals smooth absorption and emission bands in contrast to the narrow bands of crystalline silicates. However, narrow spectral emission features in the far-infrared spectra of young and old stars with circumstellar dust shells and discs obtained with the infrared space observatory (Kessler et al. 1996) indicate the presence of crystalline silicates (Waters et al. 1996). The most abundant minerals recognized are the Mg-Fe silicates, principally, end-member forsterite olivine (e.g. Waelkens et al. 1996) and enstatite pyroxene (Molster, Waters & Tielens 2002). Controversially, Bowey & Adamson (2002) have also matched the relatively smooth astronomical 10- $\mu\text{m}$  profiles with a mixture of crystalline

silicates with a relatively small component of amorphous silicate. By this analysis, the breadth of the 10- $\mu\text{m}$  features in the circumstellar discs surrounding young stars could be reproduced by a mixture of crystalline pyroxenes with varying stoichiometries (80 per cent by mass) and amorphous silicates (20 per cent).

Infrared spectra from well-characterized pyroxenes are needed for comparison with the observational data. Studies of natural terrestrial and synthetic minerals are based on ‘bulk’ techniques, where milligrams to grams of sample were analysed (e.g. Jäger et al. 1998; Chihara et al. 2002). These studies, together with single-crystal reflectance studies, are useful for estimating the compositions and quantities of silicates in astronomical environments. However, the mineralogy of bulk studies is limited by what is available at the Earth’s surface and what can be made in the laboratory. Hence, the natural samples are likely to have been formed at a very high pressure, e.g. in the Earth’s mantle, whilst the synthetics were made at atmospheric pressure, and pressure differences can substantially affect the crystal structures of the resulting minerals. The chemical environment in space and in the Earth and the laboratory is also vastly different so some astronomically relevant compositions and crystal structures are probably absent from the bulk studies.

Meteoritic grains are interesting because they may have been formed and/or processed in conditions more similar to those

\*E-mail: jeb@star.ucl.ac.uk

†Present address: Department of Earth and Planetary Sciences, Faculty of Science, Kobe University, Kobe 657-8501, Japan.

observed around young stellar objects and evolved stars. In addition, they are known to have different and differently varying chemical compositions and isotope ratios to terrestrial minerals. Therefore, they provide an opportunity to study silicates with a completely different history to those normally available. However, the quantities of material available for study are much smaller so microscopic techniques are necessary to determine their mineralogy and infrared spectra. Grain compositions are also widely varying on micrometer scales so the stoichiometry of individual grains must be determined with a scanning electron microscope (SEM).

Enstatite pyroxenes are among the most common silicates in the most primitive meteorites and interplanetary dust particles but there are few published spectroscopic measurements of extraterrestrial pyroxenes (e.g. reflectance data in Bukovanska, Nmec & Solc 1998), even though these grains probably formed in environments closer to those of the dust observed by astronomers. The best meteoritic source for primitive enstatites is type 3 chondrites. This group of meteorites has undergone only relatively small alteration since the formation of their parent bodies in the young Solar system; they are thus mineralogically highly primitive.

The most primitive grains are also the smallest (submicron- to micron-sized). To reach similar size scales we are using microspectroscopic methods which allow the measurement of individual grains down to sizes of  $10 \times 10 \mu\text{m}$  (Morlok et al. 2005, 2006). Our aim is to provide a comprehensive data base of the spectroscopic properties of the diverse mineral phases and components of meteorites for use by the astronomical and mineralogical communities. Published studies of other components include transmission spectra of pre-solar diamonds (Braatz et al. 2000), sulphides (Keller et al. 2000, 2002) and olivines (Morlok et al. 2005). Further studies were made with reflectance methods (Bukovanska et al. 1998). Similar microspectroscopic methods have also been used on interplanetary dust particles (IDPs) (Keller & Flynn 2003; Molster et al. 2003), glass with embedded sulphides (GEMS) (Bradley et al. 1999) and micrometeorites (Osawa, Kagi & Nagao 2001).

## 2 SAMPLE AND TECHNIQUES

Pyroxenes are chain silicates, characterized by chains of linked  $\text{SiO}_4$  tetrahedra along the crystallographic *c*-axis. Their generic formula is  $(\text{X}^{2+}, \text{Y}^{2+})\text{Si}_2\text{O}_6$ . The cations in the X and Y positions are mostly iron, magnesium and calcium, but these can also be substituted with sodium, manganese, lithium, aluminium chromium or titanium. Pyroxenes occur as orthorhombic and monoclinic crystals (e.g. Deer, Howie & Zussmann 1992).

In this work, we focus on pyroxenes forming a solid solution between Enstatite ( $\text{Mg}_2\text{Si}_2\text{O}_6$ ) and Ferrosilite ( $\text{Fe}_2\text{Si}_2\text{O}_6$ ). These two minerals from a solid solution in which magnesium and iron occur in the cation positions in all possible ratios. In the following, these Mg:Fe ratios are expressed as enstatite content  $\text{En}_x$ , calculated from the atomic per cent of these elements.  $\text{En}_{100}$  means pure magnesium enstatite,  $\text{En}_{70}$ , would be a pyroxene with 70 per cent of the cation positions filled with Mg and 30 per cent with iron.

### 2.1 Sample selection and preparation

Pyroxene grains were obtained from the source material used by Morlok et al. (2006) for their study of meteoritic olivines. Five different meteorites from the collections of the Natural History Museum, representing five separate parent asteroids, were selected for

study: LL3.6 ordinary chondrite Parnallee (BM34729), H/L3.6 ordinary chondrite Tieschitz (BM1975, M.11), the H3.8 ordinary chondrite Dhjala (BM1976, M12), the CV3.3 carbonaceous chondrite Vigarano (BM1920, 347) and the CO3.3 carbonaceous chondrite Ornans (BM42474). These meteorites were collected immediately after they were seen to fall, minimizing any effects from terrestrial contamination or weathering. The five meteorites are almost unshocked, with shock stages ranging from S1 to S2 (i.e. they have experienced shock pressure  $<10$  GPa). The dust which formed the meteorites has therefore been largely unaltered by heat and shock within the parent meteorite. For this study, we also took material from the EH3 Kota-Kota (BM1905.355) enstatite meteorite, which exhibits moderate shock features of Stage S4 (30–35 GPa). These were the most primitive meteorites of which substantial quantities of material were available.

Primitive meteorites are complex structures. They consist of objects like chondrules (silicate-rich spherical objects) and calcium-aluminium-rich inclusions (CAI), embedded in a fine-grained matrix. Owing to the difficulties of the separation process, it was not possible to determine from which part of the meteorite a given enstatite comes. However, given the sizes of the original grains (30 to  $100 \mu\text{m}$ ), most of them are probably from chondrules.

We followed the same sample preparation and characterization procedure also used for olivines in Morlok et al. (2006). The grains were selected according to their stoichiometry which was determined with a SEM with energy dispersive spectroscopy (EDS). In addition, each grain was checked for its homogeneity using SEM images. All grains showing zoning or contaminations with other materials were discarded. We are thus confident that the chemical compositions (and thus Mg/Fe ratios) are as exact as possible working with such samples. Grains with silicon fractions within  $\pm 5$  per cent of the ideal pyroxene composition (Deer et al. 1992) were selected for study. Occasionally, aluminium ions replace silicon from the centre of the silicate tetrahedra and/or the  $\text{Mg}^{2+}$  and  $\text{Fe}^{2+}$  sites to make pyroxenes of formula  $(\text{Mg,Fe,Al})_2(\text{Si,Al})_2\text{O}_6$ . To generate a chemical formula, we summed Al with silicon in the tetrahedral site, but if Al + Si exceeded the ideal pyroxene composition by more than 5 per cent, the excess was attributed to the  $\text{Mg}^{2+}$  and  $\text{Fe}^{2+}$  sites.

The Mg:Fe ratio of the selected grains was normalized to 100 per cent. The majority of the sampled grains contained less than an additional 2 per cent Ca; only two of the 35 grains sampled contained Ca at the 6–9 per cent level and this did not appear to affect their spectra in comparison to grains with the same Mg:Fe ratio. Since the identification is based on chemical and not structural criteria, it was not possible to determine the orthorhombic or monoclinic crystal structure of the grains. However, in type 3 chondrites, the overwhelming majority of Ca-poor pyroxenes are clinopyroxenes (Brearley & Jones 1998). The pattern of monoclinic and orthorhombic enstatites should differ in the Si–O region, but existing data from bulk studies indicate that these are small (e.g. Jäger et al. 1998; Koike et al. 2000). It should be noted that it is difficult to obtain laboratory samples of one form that is not contaminated with the other and that the degree of contamination is not always known.

### 2.2 FT-IR analysis

The infrared transmission/absorption measurements were made using a Perkin Elmer Spectrum One Fourier-transform infrared (FT-IR) microscope. Individual grains were compressed to form a sub-micron powder with a diamond compression cell, and spectra

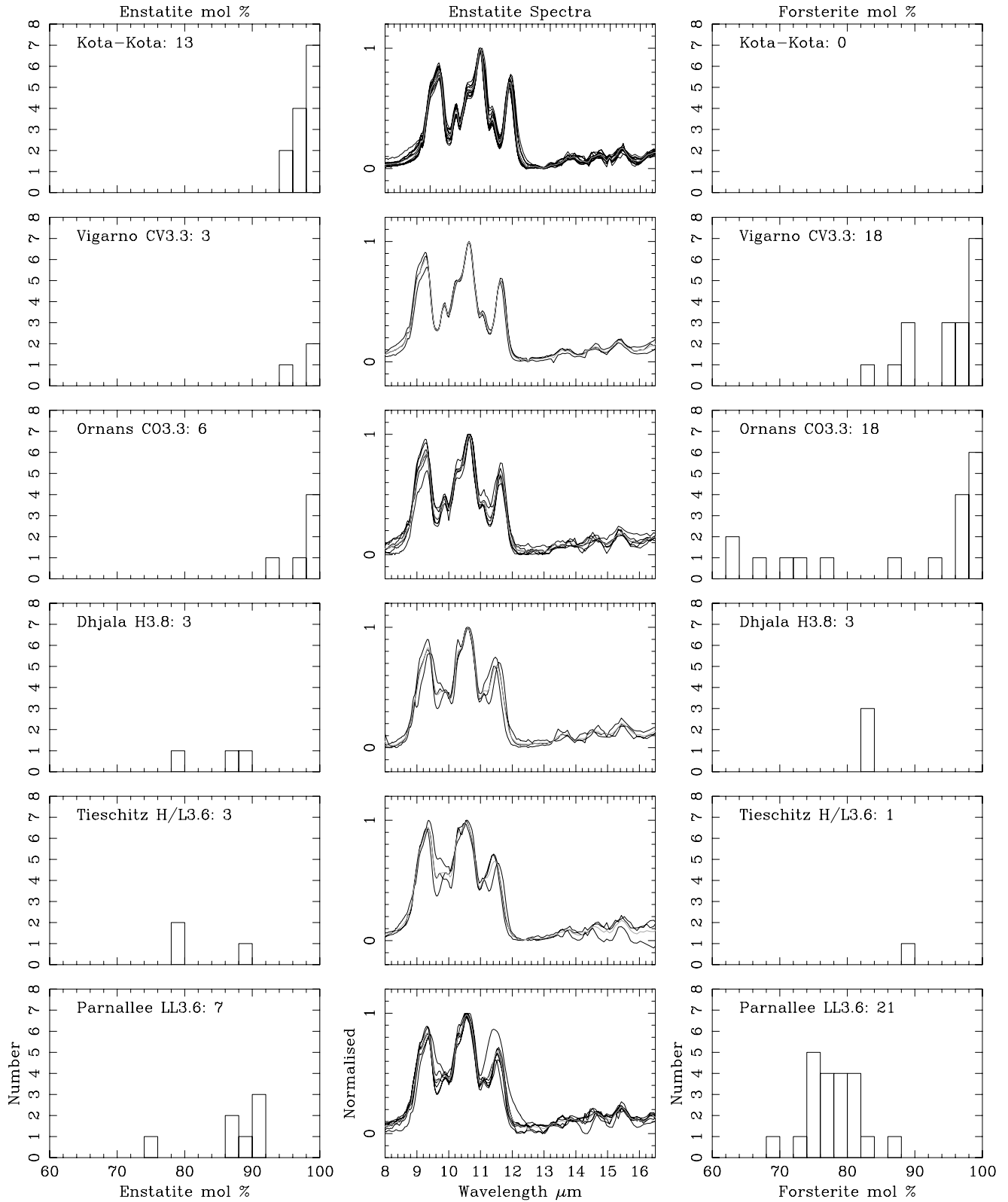


**Figure 1.** Histograms of the enstatite compositions of mineral grains obtained from each meteorite. The central panels show the spectra obtained from each enstatite grain, whilst the average is plotted in grey and the right-hand panels show the compositions of the olivine grains analysed by Morlok et al. (2006).

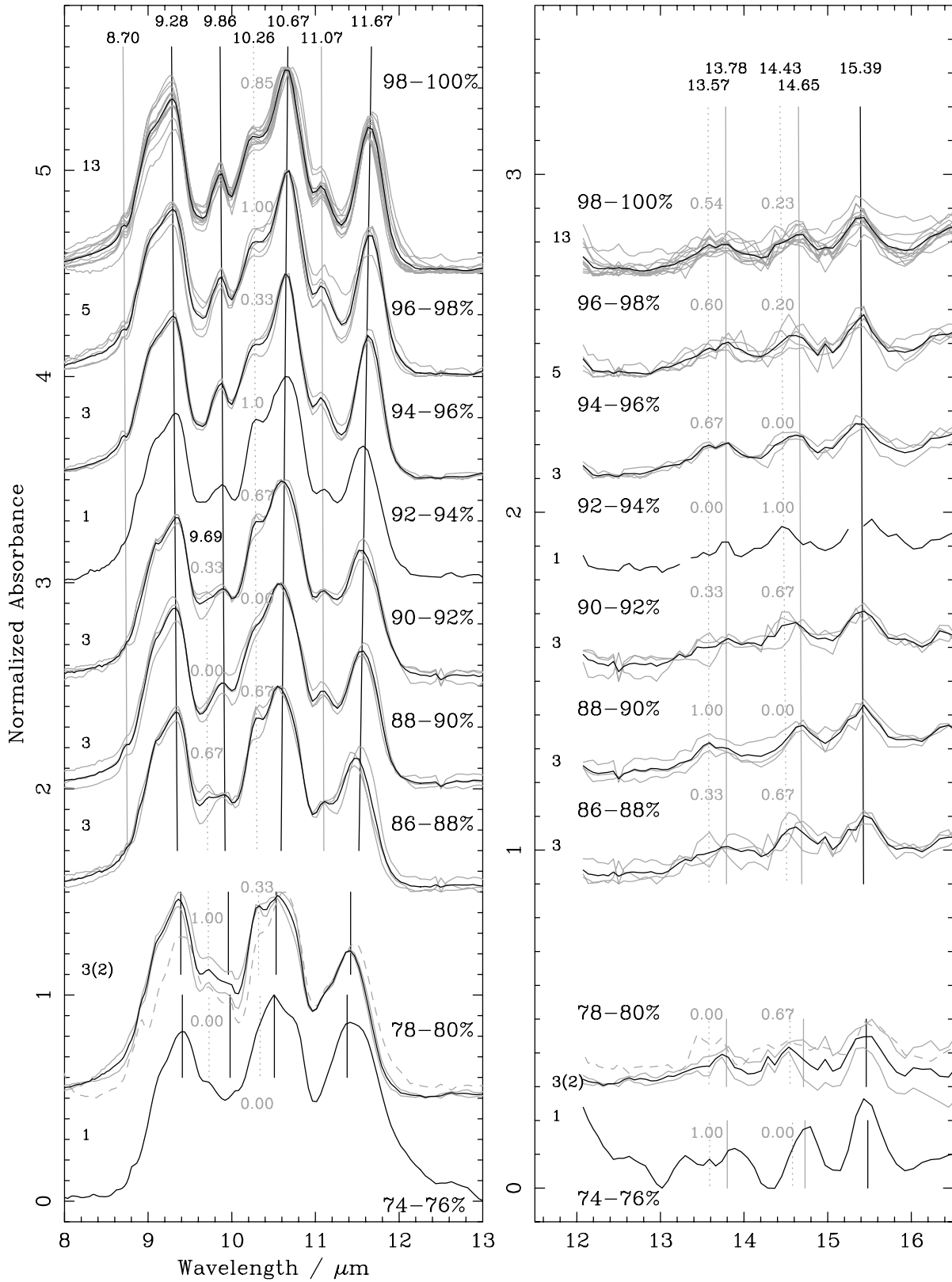


**Figure 2.** Spectra of enstatites in the compositional range from  $En_{74}$  to  $En_{100}$ . Individual spectra are plotted in grey, black curves are the average for each compositional range; the number of spectra contributing is listed at the left-hand side of each figure. The dashed spectrum in the 78–80 per cent bin was excluded from the average because of baseline problems. Solid black lines denote fitted wavelengths of the most prominent laboratory peaks, solid grey lines indicate fits to weaker peaks; dotted grey lines indicate fits to weaker peaks observed in only a few spectra, the fraction of spectra which display each of these is given in grey type.

were taken in the wavelength range from 2.5 to 16.6  $\mu\text{m}$ , at a resolution of 0.1  $\mu\text{m}$  ( $4\text{ cm}^{-1}$ ). Before a grain was compressed, a background spectrum was taken from the diamond window, on which the crushed grain was measured. More information about the techniques and sampling methods used can be found in Morlok et al. (2005, 2006).

### 3 RESULTS

#### 3.1 Compositional analyses

The compositions of the 35 analysed pyroxene grains covered the range  $\text{En}_{74}$  to  $\text{En}_{100}$ . The grain compositions cover the  $\text{En}_{86}$ – $\text{En}_{100}$  range without gaps, but the 74–76 per cent range is represented by only one grain from Parnallee, and the range 78–80 per cent by two grains from Tieschitz and one grain from Dhjala. The average enstatite composition of grains from the Enstatite chondrite, Kota-Kota, Vigarno (CV3.3) and Ornans (CO3.3) is  $\text{En}_{98}$ , whilst grains from Dhjala (H3.6), Tieschitz (H/L3.6) and Parnallee (LL3.6) are more Fe rich with mean compositions of  $\text{En}_{85}$ ,  $\text{En}_{82}$  and  $\text{En}_{87}$ , respectively. With the exception of the enstatite grains from Tieschitz (represented by only four grains), the enstatite grains were more Mg-rich than the olivine grains separated from the same meteorite (Fig. 1, and Morlok et al. 2006). In general, meteoritic pyroxenes have compositions closer to the Mg-rich end-member in comparison to olivines from the same source (e.g. Brearley & Jones 1998). We can make no true comparison of the relative numbers of enstatites and olivines in our samples because there could have been a sampling bias during the grain separation process conducted by Symes and Hutchinson. However, we observe that olivines are numerically more abundant in our mineral separates from Vigarno, Ornans and Parnallee than are the enstatites. No olivines were found in the Kota-Kota sample, more enstatites than olivines were included in the Tieschitz sample, olivines and enstatites were equally abundant in the Dhjala sample.

#### 3.2 Overview of spectra

We have identified 13 distinct peaks in the 8–16  $\mu\text{m}$  wavelength range (Fig. 2), with the strongest peaks in the 9–12  $\mu\text{m}$  range; the

identification of weaker peaks in the 12–16  $\mu\text{m}$  range is less certain because the signal-to-noise ratio is rather low for such small samples; features which looked like fringes were excluded from the analysis. The peak positions were determined using an automated peak fitting procedure of the Perkin Elmer Software used for measurements of the spectra. The 13 main features and some peaks which were observed in only a few grains are listed in Table 1, with an indication of their relative strength. The wavelengths of most bands vary slightly with the ratio of  $\text{Mg}^{2+}$  to  $\text{Fe}^{2+}$  because of the different sizes of the cations (e.g. Jäger et al. 1998; Chihara et al. 2002). Therefore, in Fig. 2 and the following discussion, we refer to bands by their fitted wavelength in  $\text{En}_{100}$ . Most bands move to higher wavenumbers (lower wavelengths) with increasing magnesium ratios, but there are cases of shifts in the other direction (Chihara et al. 2002). In general, the bands of grains nearer to the  $\text{En}_{100}$  end-member composition are sharper than those with a higher proportion of Fe; presumably this is also a consequence of the different sizes of the cations occupying similar lattice sites.

The strongest bands occur in all the sampled grains, their  $\text{En}_{100}$  wavelengths are 9.28, 9.86, 10.67 and 11.67  $\mu\text{m}$ . Weaker peaks occur between these bands at 8.70, 9.02 (shoulder), 9.69, 10.26 and 11.07  $\mu\text{m}$ . These features are confirmed by literature data. Bands in the 12–16  $\mu\text{m}$  range at 13.57, 13.78, 14.43, 14.65 and 15.39 are also confirmed by earlier studies. The very weak 13.28- $\mu\text{m}$  band may be an artefact.

#### 3.3 Mg:Fe ratio dependence of wavelength shifts

The feature positions are plotted as a function of Mg:Fe ratio in Fig. 3. In order to determine the average band position for a given composition, linear fits of band position as a function of enstatite composition have been calculated; there is a good correlation between wavelength and composition in the 8–12  $\mu\text{m}$  range. However, the correlation coefficients obtained for the  $\text{En}_{100}$  bands at 13.28, 13.57 and 13.78  $\mu\text{m}$  are very poor ( $R^2 \lesssim 0.04$ ) because the features are very weak and the fitted wavelength shifts are very small in comparison to the spectral resolution ( $<1/10$  of a resolution element) over the  $\text{En}_{75}$ – $\text{En}_{100}$  range.

**Table 1.** Fitted regression lines and correlation coefficients for the 35 enstatite grains sampled. The total compositional range was  $\text{En}_x$  where  $74.44 \leq x \leq 100$ .

$\lambda(\text{En}_{100})$ ( $\mu\text{m}$ )	$\lambda(\text{En}_{75})$ ( $\mu\text{m}$ )	Relative strength	No. of grains	Fit = $\lambda(\text{En}_0) + mx$ ( $\mu\text{m}$ )	$R^2$	$\text{En}_x$ (per cent)
13 main peaks						
8.70	8.79	Weak	22	$9.0610 - 0.0036x$	0.63	>87?
9.28	9.40	Strong	35	$9.7627 - 0.0048x$	0.78	All
9.69	9.73	Weak	6	$9.8583 - 0.0017x$	0.49	<92
9.86	9.99	Medium	35	$10.371 - 0.0051x$	0.71	All
10.26	10.34	Medium	23	$10.554 - 0.0029x$	0.31	All
10.67	10.51	Strong	35	$10.028 + 0.0064x$	0.66	All
11.07	11.14	Medium	31	$11.339 - 0.0027x$	0.40	>86
11.67	11.38	Strong	35	$10.501 + 0.0117x$	0.87	All
13.57	13.58	Weak	18	$13.621 - 0.0005x$	0.04	–
13.78	13.80	Weak	25	$13.850 - 0.0007x$	0.02	All
14.43	14.58	Medium	11	$15.028 - 0.0060x$	0.73	All?
14.65	14.73	Medium	24	$14.933 - 0.0028x$	0.24	All
15.39	15.48	Medium	34	$15.747 - 0.0036x$	0.33	All
Peaks observed in a few grains of different composition						
9.02	9.19	Shoulder	5	$9.6732 - 0.0065x$	0.88	–
12.47	12.60	Very weak	4	$12.981 - 0.0051x$	0.85	–
13.28	13.29	Very weak	9	$13.341 - 0.0006x$	0.02	Artefact?

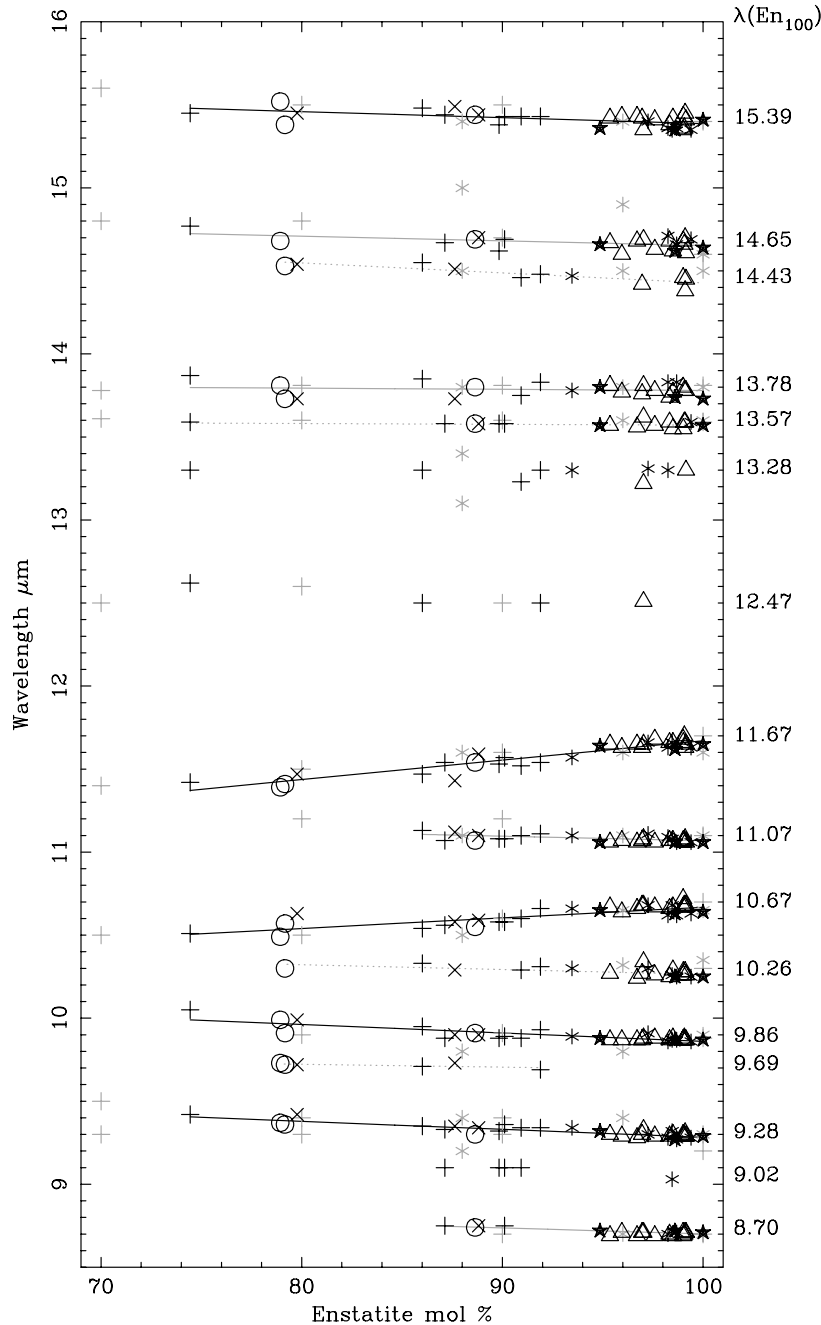


**Figure 3.** Relationship between feature wavelength and enstatite composition. Black symbols are data from this study: Kota-Kota ( $\Delta$ ) Parnallee (+), Ormans (\*), Vigarano (\*), Tieschitz ( $\circ$ ), Dhjala ( $X$ ). Grey symbols denote the literature data: Chihara et al. 2002 (+), Jaeger et al. 1998 (\*). Linear fits to the data are plotted where appropriate. Solid black lines denote fitted wavelengths of the most prominent laboratory peaks, solid grey lines indicate fits to weaker peaks, dotted lines indicate fits to the additional peaks which occur in the least common spectra for each composition.

In general, the wavelength of the band increases with the proportion of Fe. However, the wavelengths of the strong bands at 10.67 and 11.67 *decrease* with increasing Fe content. The 11.67- $\mu\text{m}$  band exhibits the largest compositional wavelength shift (twice as large as any other). The fit to the 11.67- $\mu\text{m}$  band can be applied to the averaged spectra of each meteorite (Fig. 1), and the derived mean Mg:Fe ratio is within  $\pm 1$  per cent of the average compositions obtained in the SEM analyses given in Section 3.1.

Previous studies (Jäger et al. 1998; Chihara et al. 2002) do not find a shift in the 9.86- and 13.57- $\mu\text{m}$  bands with Fe content. However,

whilst this is true for the 13.57- $\mu\text{m}$  band, we find that the 9.86- $\mu\text{m}$  band shifts to 9.99  $\mu\text{m}$  in  $\text{En}_{75}$ . The previous studies measured the 9.02- $\mu\text{m}$  shoulder and the weak 9.69- $\mu\text{m}$  peak only in samples with more Fe than the  $\text{En}_{75}$ – $\text{En}_{100}$  range studied here.

### 3.4 Infrequently observed bands

The weak peak at 8.70  $\mu\text{m}$  and the medium peak at 11.07  $\mu\text{m}$  are seen only in grains with Mg in excess of 87 per cent and the 9.69- $\mu\text{m}$  feature has been measured only in grains with less than

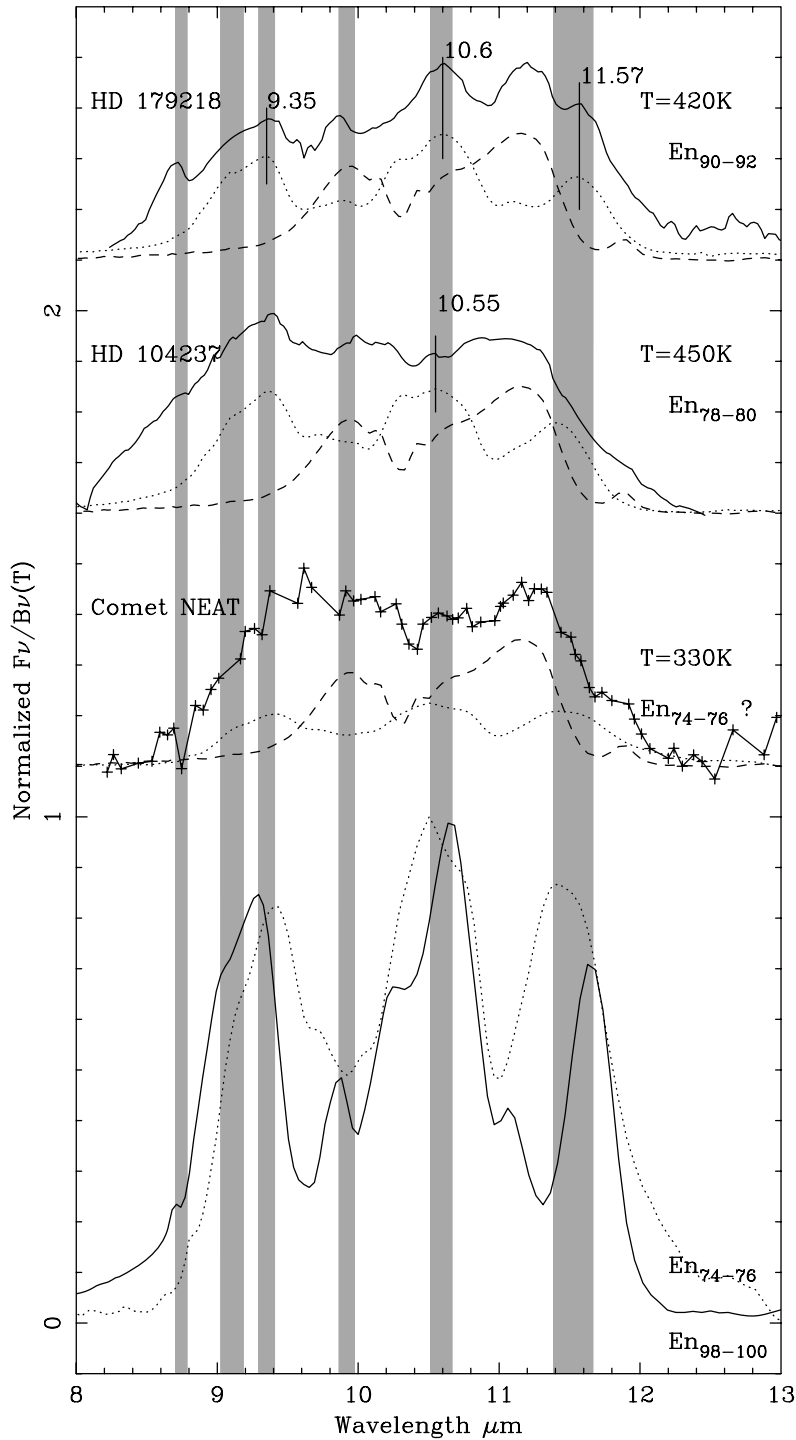


**Figure 4.** Comparison of  $\text{En}_{100}$  (lowest solid curve) and  $\text{En}_{74}$  (lowest dotted curve) meteoritic grains with the astronomical emission features of dust surrounding the Herbig AeBe stars HD 179218 and 140237 (van Boekel et al. 2005) and C/2001 Q4 (NEAT) (Wooden et al. 2004). Grey bars indicate the fitted band positions of the most prominent peaks in the measured  $\text{En}_{74}$ – $\text{En}_{100}$  grains. The astronomical flux ( $F_\nu$ ) spectra have been divided by a blackbody [ $B_\nu(T)$ ] of temperature  $T$ , where  $T$  is chosen so that the scaled flux of the blackbody is equal to that observed at 8 and 13  $\mu\text{m}$ . The spectra of  $\text{Fo}_{100}$  (dashed) and the best matching averaged enstatite,  $\text{En}_x - y$ , composition (dotted) are compared with each observation. Vertical bars with wavelengths indicate the positions of astronomical bands used to identify the composition of the best meteoritic match.

92 per cent Mg. However, the existence of peaks at 10.26 and 14.43  $\mu\text{m}$  do not seem to depend on composition. Variation between individual spectra of similar composition may also depend on crystal structure (e.g. monoclinic or orthorhombic) or orientation in the crushed samples, but much more study is required to determine their origin.

## 4 DISCUSSION

### 4.1 Comparison with astronomical observations

Observations of distinctive crystalline features in the 8–13  $\mu\text{m}$  range are rare. Spectral identification of crystalline silicates from



ground-based telescopes is hampered by the presence of strong 9.4–9.8  $\mu\text{m}$  absorption features resulting from ozone in the Earth's atmosphere and rapid changes in the atmosphere's opacity because of fluctuations in the proportions of water vapour.

10- $\mu\text{m}$  observations of objects with far-infrared forsterite bands are frequently affected by the presence of strong narrow features identified with polyaromatic hydrocarbons which occur a range of wavelengths close to 7.7, 8.7, 11.0 and 11.3  $\mu\text{m}$  (e.g. Molster et al. 2001). The minerals identified in the far-infrared are unlikely to be seen at 10  $\mu\text{m}$  because they have very low emission temperatures ( $\sim 100$  K) compared to 200–600 K typical of 10- $\mu\text{m}$  silicate emission.

Our spectra of meteoritic enstatites are compared with astronomical spectra known to be rich in crystalline pyroxenes in Fig 4. HD 179218 and 104237 are two of the most enstatite-rich 10  $\mu\text{m}$  optically thin Herbig AeBe stellar emission spectra observed to date (van Boekel et al. 2005). Crystalline olivine and orthopyroxene have been identified in the spectrum of Oort Cloud Comet C/2001 Q4 (NEAT) as it entered the inner Solar system. The crystalline olivine bands are at 10.0 and 11.2  $\mu\text{m}$  with weak peaks at 10.5 and 11.8  $\mu\text{m}$ , crystalline orthopyroxenes are identified with bands at 9.3 and 10.5  $\mu\text{m}$  (Wooden, Woodward & Harker 2004). We cannot estimate the Mg:Fe ratio in the olivine grains because the compositional wavelength shift is too small (0.09  $\mu\text{m}$  for the shift of the 11.21  $\mu\text{m}$   $\text{Fo}_{100}$  feature to 11.30  $\mu\text{m}$  in  $\text{Fo}_{60}$ ; Morlok et al. 2006) in comparison to the spectral resolution of the astronomical observations (0.06–0.2  $\mu\text{m}$ ). The peak positions in the astronomical observations were measured 'by eye' with a cursor because they are much weaker than the laboratory peaks. Our fits of the linear dependence to the laboratory peaks indicate that the 9.35, 10.60 and 11.57 bands of HD 179218 are matched by a pyroxene composition of  $\text{En}_{90-92}$ , and the 10.55- $\mu\text{m}$  band of HD 104237 is matched by a composition of  $\text{En}_{78-80}$ . The less distinct, broader peaks in the lower signal-to-noise spectrum of comet NEAT could be represented by a composition of  $\text{En}_{74-76}$ . If these simplistic comparisons with the astronomical grains are correct (they do not consider the detailed effects of blending with other silicates, differences in grain temperature or the effects of grain shape), then the pyroxenes seen in these environments are more Fe-rich than are the forsterite ( $\text{Fo}_{100}$ ) grains identified in the far-infrared which are found to be Mg end-member grains (e.g. Bowey et al. 2002).

## 5 SUMMARY

Mid-IR spectra from enstatite grains, separated from primitive type 3 meteorites, have been taken with microspectroscopic FT-IR techniques. From the results, representative band position was calculated based on regression lines. In general, the wavelength of the band increases with the proportion of Fe. However, the wavelengths of the strong bands at 10.67 and 11.67  $\mu\text{m}$  decrease with increasing Fe content. The 11.67- $\mu\text{m}$  band exhibits the largest compositional wavelength shift (twice as large as any other).

Our fits of the linear dependence of the pyroxene peaks indicate that the crystalline pyroxene peaks in the 10- $\mu\text{m}$  spectra of Herbig AeBe stars HD 179218 and 104237 are matched by pyroxenes of about  $\text{En}_{90-92}$  and  $\text{En}_{78-80}$ , respectively. If these simplistic com-

parisons with the astronomical grains are correct, then the enstatite pyroxenes seen in these environments are more Fe-rich than are the forsterite ( $\text{Fo}_{100}$ ) grains identified in the far-infrared which are found to be Mg end-member grains. This differs from the general composition of type 3 chondritic meteoritic grains in which the pyroxenes are more Mg-rich than are the olivines from the same meteorite (Brearley & Jones 1998).

## ACKNOWLEDGMENTS

We thank R. F. Symes and R. Hutchison for the mineral separates. Financial support from the PPARC to AM, JEB and MMG, and from the EU Marie Curie Programme for MK is gratefully acknowledged. This paper is IARC Contribution No. 2005-99. JEB acknowledges AM Woodcraft and an absence of research funding for delaying the publication of this paper.

## REFERENCES

- Bowey J. E., Adamson A. J., 2002, MNRAS, 334, 94  
 Bowey J. E. et al., 2002, MNRAS, 331, L1  
 Braatz A., Ott U., Henning T., Jäger C., Jeschke G., 2000, Meteorit. Planet. Sci., 35, 75  
 Bradley J. P. et al., 1999, Sci, 285, 1716  
 Brearley A. J., Jones R. H., 1998, in Papike J. J., ed., Mineralogical Soc. of America Rev. in Mineralogy Vol. 36, Planetary Materials. Mineralogical Soc. of America, Washington, DC, p. 3.1  
 Bukovanska M., Nmec I., Solc M., 1998, Meteorit. Planet. Sci., 33, A25  
 Chihara H., Koike C., Tsuchiyama A., Tachibana S., Sakamoto D., 2002, A&A, 391, 267  
 Deer W., Howie R., Zussmann J., 1992, An Introduction to the Rock-Forming Minerals. Addison Wesley Longman Ltd., Essex  
 Jäger C., Molster F., Dorschner J., Henning T., Mutschke H., Waters L., 1998, A&A, 339, 904  
 Keller L. P., Flynn G. J., 2003, Lunar and Planet. Inst. Conf. Abstracts, 34, 1903  
 Keller L. P., Bradley J. P., Bouwman J., Molster F. J., Waters L. B. F. M., Henning G. J. F. T., Mutschke H., 2000, Lunar and Planet. Inst. Conf. Abstracts, 31, 1860  
 Keller L. P. et al., 2002, Nat, 417, 148  
 Kessler M. F. et al., 1996, A&A, 315, L27  
 Koike C. et al., 2000, A&A, 363, 1115  
 Molster F. J. et al., 2001, A&A, 372, 165  
 Molster F. J., Waters L. B. F. M., Tielens A. G. G. M., 2002, A&A, 382, 222  
 Molster F. J., Demyk A., D'Hendecourt L., Bradley J. P., 2003, Lunar and Planet. Inst. Conf. Abstracts, 34, 1148  
 Morlok A., Köhler M., Bowey J. E., Grady M. M., 2005, Planet. Space Sci., 54, 599  
 Morlok A., Bowey J. E., Köhler M., Grady M. M., 2006, Meteorit. Planet. Sci., 41, 773  
 Osawa T., Kagi H., Nagao K., 2001, Antarct. Meteorit. Res., 14, 71  
 van Boekel R., Min M., Waters L. B. F. M., de Koter A., Dominik C., van den Ancker M. E., Bouwman J., 2005, A&A, 437, 189  
 Waters L. B. F. M. et al., 1996, A&A, 315, L361  
 Waelkens C. et al., 1996, A&A, 315, L245  
 Wooden D. H., Woodward C. E., Harker D. E., 2004, ApJ 612, L77

This paper has been typeset from a  $\text{T}_{\text{E}}\text{X}/\text{L}_{\text{A}}\text{T}_{\text{E}}\text{X}$  file prepared by the author.